# Evaluating accessibility of intravenously administered nanoparticles at the lesion site in rat and pig contusion models of spinal cord injury

**Yue Gao**[1], **Sivakumar Vijayaraghavalu**[1], **Melinda Stees**[1], **Brian K. Kwon**[2], and **Vinod Labhasetwar**[1,*]

[1]Department of Biomedical Engineering, Lerner Research Institute, Cleveland Clinic, Cleveland, OH 44195, USA

[2]Department of Orthopedics, International Collaboration of Repair Discoveries (ICORD), University of British Columbia, Vancouver, BC, Canada

## Abstract

In spinal cord injury (SCI), timely therapeutic intervention is critical to inhibit the post-injury rapidly progressing degeneration of spinal cord. Towards that objective, we determined the accessibility of intravenously administered biodegradable nanoparticles (NPs) as a drug delivery system to the lesion site in rat and pig contusion models of SCI. Poly (D,L-lactide *co*-glycolide, PLGA)-based NPs loaded with a near-infrared dye as a marker for NPs were used. To analyze and quantify localization of NPs to the lesion site, we mapped the entire spinal cord, segment-by-segment, for the signal count. Our objectives were to determine the NP dose effect and duration of retention of NPs at the lesion site, and the time window post-SCI within which NPs localize at the lesion site. We hypothesized that breakdown of the blood-spinal cord barrier following contusion injury could lead to more specific localization of NPs at the lesion site. The mapping data showed a dose-dependent increase and significantly greater localization of NPs at the lesion site than in the remaining uninjured segment of the spinal cord. Further, NPs were seen to be retained at the lesion site for more than a week. With delayed post-SCI administration, localization of NPs at the lesion site was reduced but still localize even at four weeks post-injury administration. Interestingly, in uninjured animals (sham control), greater accumulation of NPs was seen in the thoracic and lumbar enlargement regions of the spinal cord, which in animals with SCI changed to the lesion

site, indicating drastic post-injury hemodynamic changes in the spinal cord. Similar to the rat results, pig contusion model of SCI showed greater NP localization at the lesion site. In conclusion, NPs could potentially be explored as a carrier for delivery of therapeutics to the lesion site to minimize the impact of post-SCI response.

## Keywords

CNS Injury; Drug Delivery; Nanocarriers; Biodegradable Polymers; Sustained Release; Imaging

## INTRODUCTION

Devastating motor, sensory, and autonomic dysfunctions give rise to long-term personal hardship for the survivors of traumatic spinal cord injury (SCI) [1]. The pathophysiology of traumatic SCI involves primary and secondary injury [2]. The primary injury is the immediate destruction of spinal cord tissue at the lesion site. The damaged and necrotic cells at the site of primary injury [3] activate a secondary injury cascade [4, 5], which has an acute, an intermediate and a chronic phase. While the exact time frames for each of these phases are not delineated, in general, there is a progression of pathophysiologic responses in the hours to days after the injury that can worsen the tissue damage as part of the "secondary injury" cascade (Figure 1) [6–8]. It is postulated that the long-term outcome of traumatic SCI significantly depends on the ability of exogenous treatments to prevent the progression of secondary injury cascade within this therapeutic window [9, 10]. During the chronic phase, delivery of therapeutics to the lesion site could facilitate axonal regeneration for neuronal connectivity and functional recovery [11]. Towards the above objective, we have been investigating intravenously injectable biodegradable nanoparticles (NPs) as a drug delivery system.

The purpose of this study was to evaluate the effect of different parameters and conditions that are critical for localization of intravenously injected NPs at the lesion site in a rat contusion model of SCI and then confirming the key outcome within the larger spinal cord of a pig contusion model of SCI. While rat model of SCI is relatively inexpensive and easy to evaluate for therapeutic efficacy, it is essential to demonstrate efficacy in a large animal model of SCI for clinical translation of therapy. In this regard, pig model of SCI is well suited as its spinal cord is comparable in size to that of humans [12]. We used near-infrared (NIR) dye-loaded NPs and developed a new optical imaging method to quantitatively map the entire spinal cord, segment-by-segment, for the signal count that can be correlated to the NP amount localized. Our objectives were to determine: **a)** the effect of dose of NPs injected on their localization at the lesion site with respect to the entire spinal cord; **b)** duration of retention of NPs at the lesion site following a single-dose injection; and **c)** the time window post-SCI within which the administered NPs localize at the lesion site. We hypothesized that intravenously administered NPs are accessible more at the lesion site than in the remaining uninjured segment of the spinal cord due to breakdown of the blood-spinal cord barrier (BSCB) at the lesion site. The results of these studies are critical for exploring NPs effectively as a drug delivery system for treating acute SCI.

# MATERIALS AND METHODS

## Materials:

Poly (D,L-lactide *co*-glycolide) (PLGA; 50:50, inherent viscosity of 0.76–0.94 dL/g) was purchased from LACTEL Absorbable Polymers (Birmingham, AL). Poly (vinyl alcohol) (PVA; 87–90% hydrolyzed, mol. wt. 30,000–70,000), Bovine Serum Albumin (BSA), Dimethyl tartaric acid (DMT) and glucose were purchased from Sigma-Aldrich (St. Louis, MO). Near-infrared (NIR) dye (SDB5700) was obtained from H.W. Sands Corp. (Jupiter, FL). Chloroform was obtained from Fisher Scientific (Pittsburgh, PA).

## Formulation of NPs:

These were formulated by a double water-in-oil-in-water (w/o/w)emulsion solvent-evaporation method. In brief, BSA solution in water (10% w/v, 300 μL) was emulsified into a polymer solution containing 81 mg PLGA (with 9 mg DMT) and 250 μg of NIR dye in 3 mL chloroform. The primary w/o emulsion was formed, first by vortexing for 1 min followed by sonication for 2 min on an ice bath using a stepped microtip probe at 40% power (Qsonica LLC, Model Q500, Newtown, CT). BSA was used as a model protein because of our interest in developing protein-based neuroprotective therapy [13, 14] and DMT as an inert plasticizer. As described in our previous study, DMT is unique in that it is soluble in both aqueous and organic solvents, and forms pore in the PLGA matrix, thus preventing accumulation of acidic oligomers within NPs that are formed as a result of polymer degradation; these acidic oligomers if remained entrapped can potentially denature proteins [15]. Also, because DMT forms pores, it helps in the release of the encapsulated protein in a sustained manner [16]. The above w/o emulsion was emulsified into 18 mL of 3% w/v PVA solution in water, first by vortexing for 1 min followed by sonication as above for 4 min to form multiple (w/o/w) emulsion. The PVA solution used for emulsification was prepared by sprinkling PVA slowly into water while stirring on a magnetic stir plate at room temperature and then warmed to ~ 80 °C to facilitate its further dissolution; the solution was then cooled to room temperature and filtered through 0.22 μm pore filtration flask (Millipore, Billerica, MA). The emulsion was stirred overnight (~18 hrs) on a magnetic stir plate at 1,000 rpm in a fume hood at room temperature with an airflow set at a face velocity of 200 feet/min (6,400 cm/min). The formed NP dispersion was stirred for an additional one hr in a desiccator under vacuum (at ~ 23 psi) to ensure the removal of chloroform. The NPs formed were recovered by ultracentrifugation at 30,000 rpm (82,000 x g) (Optima XE-90 with a 50.2Ti rotor, Beckman Coulter, Brea, CA) for 30 min. The supernatant was discarded, and the pellet was resuspended in autoclaved Milli-Q water (ASTM Type 1 water, EMD Millipore Super-Q Plus filtration system; EMD Millipore, Darmstadt, Germany). The above process of centrifugation and resuspension of NPs was repeated two times to remove excess PVA, as well as the unencapsulated BSA and dye. After a final re-suspension and sonication of the pellet as above, it was centrifuged at 1,000 rpm (216 x g) for 10 min (Thermo Electron Sorvall legend RT Plus centrifuge, Thermo Scientific, Waltham, MA) to remove large aggregates, if any. The supernatant was collected to which glucose was added as a cryoprotectant (2% w/v of NP suspension, volume of NP suspension = 20 ml or ~1:4 w/w NPs to Glucose). Appropriate aliquots of the NP dispersion were made in pre-weighted cryovials (Nunc, Roskilde, Denmark) and then the samples in vials were frozen at −80 °C in

a freezer. The samples were lyophilized in a Freezone 4.5 (Labconco, Kansas City, MO) for 2 days (0.016mBar, −55 °C). The added glucose before lyophilization helps in re-dispersing NPs in saline without requiring sonication before injecting to animals. To estimate the NP amount in each vial, few representative vials containing aliquots of NP suspension with and without added glucose were lyophilized and weighted. The average difference in the weight was used to calculate the NP amount in each vial. The vials were stored at −20 °C until used for animal studies.

### Characterization of NPs:

Size and zeta potential of NPs were determined using NICOMP 380 ZLS (Particle Sizing Systems, Port Richey, FL). Measurements were made on the NP dispersions prepared by sonication as above at ~1 mg NPs/mL in water.

## ANIMAL STUDIES

### Rat model of SCI:

The Cleveland Clinic's Institutional Animal Care and Use Committee approved all animal procedures, and these were carried out according to the Federal and internal guidelines. Sprague-Dawley rats of age 6 to 8 weeks were obtained from Envigo (Cleveland, OH). Each group contained an equal number of male and female rats. Animals were housed in a temperature- and light-controlled room on a 12-hr light, 12-hr dark cycle with free access to water and food. Following laminectomy under gas anesthesia (isoflurane 2–4%), the spinal cord was exposed at T10. The SCI was induced using Infinite Horizon (IH) impactor (Mode IH-0400, Precision Systems and Instrumentation, LLC, VA) with an impact force of 250 Kdyn and a speed of 100 mm/s with a dwelling time of 15 sec. As per the manufacturer of the impactor, these conditions are set to induce a "severe" contusion SCI. Bladder expression was performed manually twice daily during the first postoperative week, then once daily in the second wk or until spontaneous voiding was confirmed. Animals were monitored for signs of urinary tract infection such as urine color, content (blood or pus) and consistency. Animals' weight was also recorded pre- and post-injury at a regular time interval.

### Administration of NPs:

Following SCI, NPs dispersed in sterile normal saline were administered through tail vein at specified time points and doses. The injection volume was kept constant to 0.8 mL whereas the concentration of NPs was altered depending upon the protocol dose. Just before injection, NPs were dispersed by adding a required volume of saline followed by gentle vortexing. In one group of animals, different doses of NPs (15, 30 and 60 mg/kg) were administered at 6 hrs post-injury to determine the dose effect on localization of NPs at the lesion site whereas in another group, a dose of 30 mg/kg was administered at 1, 2, and 4 wks post-injury to determine how post-injury time delay influences NP localization at the lesion site. The 6-hr post-injury NP administration time point was taken from the above dose-response study. Animals in all the above groups were euthanized at 24 hrs after the injection of NPs. In another group, NPs were administered (dose = 30 mg/kg) at 6 hrs post-injury, and the animals were euthanized at 1 wk post-NP injection. The 1-day retention time point was

taken from the above dose-response study to compare with the 1-wk time point. In the sham control group, NPs (dose = 30 mg/kg) were injected 6 hrs after performing laminectomy but without inducing SCI and the animals were euthanized 1 day after injecting NPs.

### Harvesting of spinal cord:

Animals were euthanized and the blood was drained via cardiac puncture followed by perfusion with normal saline. Laminectomy was performed to expose the entire spinal cord from foramen magnum to sacrum and was then removed by severing at all nerve roots with a micro scissor before cut off at the base of the skull. Spinal cords were kept at −80 °C until taken for analysis.

### Mapping of the spinal cord for the signal count:

The dye incorporated in NPs can be imaged in the near infrared region (NIR); it provides a strong and stable signal. Since the dye is hydrophobic and used at a very low concentration (~0.3% w/w polymer weight), it's leaching from NPs is minimum under sink condition, and hence acts as a marker for NPs. Previously, we have determined that the dye leaching from NPs is insignificant, with a cumulative release of ~1.5% in 12 hrs, 2.5% in 48 h, and 3% in 96 h, almost reaching to a plateau release phase with time when incubated in 1% bovine serum albumin (used to create sink condition) solution in PBS [17]. In our previous study, these dye loaded NPs were used to determine their biodistribution in animal models of the tumor [17], and also to study their transport across the skin layers in an *ex vivo* experiment [18]. The NP-specific signal in the NIR region could be quantified by appropriately setting the spectral parameters without the interference from the tissue background signal, which is insignificant in the NIR region.

The harvested spinal cords stored at −80 °C were thawed and kept on an ice bath in the dark until taken for imaging using the Maestro Optical Imaging System (Version 3.0.1, Caliper Life Sciences, Hopkinton, MA). They were then placed on a non-fluorescent blackboard positioned at stage 1A of Maestro. We confirmed that freezing and thawing of spinal cords do not affect the NP-specific signal count. The exposure protocols involved two filters: Blue filter (wavelength 500–720 nm) and NIR filter (wavelength 740–950 nm). The dye incorporated in NPs shows a peak at 770 nm. The blue filter was used for visual imaging of the spinal cord whereas the NIR filter for the detection of NPs localized in the spinal cord. The exposure time was optimized to 6200 ms so that the signal due to NPs is not saturated. The images obtained with blue and NIR filers were co-localized for visualization of both the spinal cord and the signal due to NPs. After un-mixing the spectra to separate the NIR dye signal from the tissue background signal, the co-localized images were analyzed segment-by-segment (virtual segmental analysis using Maestro Software) with each segment of $7 \times 2$ mm (sectional x axial) as the regions of interest (ROI). A total of ~35 ROIs were applied to complete the "mapping" of the entire spinal cord for an average signal count for each ROI. To enhance the visual effect, heat-maps were created to illustrate relative signal intensity due to the NPs localized in different segments of the spinal cord. After mapping, spinal cords were cut and the cross sections were imaged for NP signal as above.

### Correlating signal count to NP amount in spinal cord:

The spinal cords harvested as above from normal rats (uninjured and did not receive NPs) were weighed and suspended in RIPA lysis and extraction buffer (ThermoFisher Scientific) at 100 mg/mL and homogenized using Minilys Homogenizer (Bertin Technologies, Rockville, MD). The homogenization of spinal cords was carried out in two cycles, with each cycle lasting for 2 min, after a gap of 2 min, with the samples kept on an ice bath between the cycles to avoid their overheating during homogenization. The tissue homogenate (300 μL) was then added into wells of a black non-fluorescent 96-well plate (BRAND Plates, Wertheim, Germany). Unlike in a transparent plate, black opaque plate prevents interference of the sample signal from one well to another. The homogenized tissue samples were loaded into 20 wells that are in the center part of the plate (C4–8 to F4–8 or leaving three on left and right and two on top and bottom empty). Based on our prior experience, thesame sample when loaded into these wells produces a consistent signal. This is because thesignal reflected from these samples, which is captured by the camera located above the plate, is less affected by the angle at which the laser focuses onto these wells.

A stock suspension of dye-loaded NPs (2 mg/mL) was prepared in saline as above and was added to the tissue homogenate in wells so that the NP amount ranges from 0 to 40 μg. Since the volume of NP suspension added is insignificant in comparison to the total volume of spinal cord homogenate in each well (0.06% change in volume at 40 μg NP amount), it is not expected to cause significant dilution effect with increasing amounts of NPs added to the wells. The NP-tissue homogenate mixture was pipetted repeatedly for uniform mixing, taking care that no air bubbling occurs. The plate was imaged using Maestro, and the signal count was measured at an exposure time of 500 ms which was automatically detected optimal by the instrument for the loaded samples. A standard plot was created between the NP amount and the signal count. The spinal cords from the experimental group that received 30 mg/kg NP dose at 6 hr post-SCI and harvested at 1-day post-NP administration, after mapping for the signal count, were processed and analyzed as above to determine the total NP amount present in the entire spinal cord. A factor was calculated correlating the area under the curve (AUC) from the mapping data and the amount of NP present in the entire spinal cord as determined from the standard plot in the spinal cord homogenate. This factor was used to determine the NP amount present at the lesion site from the AUC for those segments (21 to 26) obtained from the mapping data. The AUC values from the mapping data were used to determine the NP amount localized in the entire spinal cord, certain segments of the spinal cord, or in different treatment groups.

### Localization of NPs in pig contusion model SCI:

Because the delivery and biodistribution of a therapeutic within the spinal cord are quite likely to be influenced by the size of the spinal cord, we sought to confirm localization of NPs at the lesion site in a pig contusion model of SCI [19]. In brief, female Yucatan miniature pigs (Memorial University of Newfoundland, Canada and Sinclair Bio-resources, Columbia, MO) weighing 20–25 kg were used. All pre-surgical and post-surgical procedures were followed as per the guidelines of the Canadian Council on Animal Care (CCAC) and after institutional ethics approval. A dorsal laminectomy was performed from T9 to T12 to expose the dura and spinal cord. The weight drop guide-rail apparatus was fixed to the

thoracic spine at T9–T11, and the 50 g impactor was dropped along the rail from a height of 20 cm to rapidly strike the exposed spinal cord at T10. Immediately after the contusion impact, a 100 g weight was gently lowered onto the impactor, and this 150 g weight was left in place to compress the cord for 5 min. Animals received a dose of 6 mg/kg dye-loaded NPs which is equivalent to 30 mg/kg NP dose used in the above rat study. This dose was calculated using the correction factor (Km), which is based on weight/surface area values for different species of animals [20]. One animal received the NP dose at 3 hrs post-injury and it was euthanized at 2 hrs post-NP-infusion whereas the second animal received the NP dose at 30 min post-injury and spinal cord was harvested at 5 hrs post-NP injection. Due to its long length, the entire spinal cord could not be placed onto the Maestro stage for mapping. Therefore, longitudinal slices of the spinal cord representing the lesion site at T10 and uninjured sites from R1 to R2 and C1 to C2 representing the rostral and caudal areas respectively were taken for imaging using Maestro as above.

### Statistical Analysis:

Data are shown as mean ± s.e.m. Statistical analysis was performed using Prism 6 for one-way analysis of variance (ANOVA) or Students t-test to assess differences between groups. p 0.05 was considered significant.

## RESULTS

### Physical characterization of NPs:

Mean hydrodynamic diameter of the dye-loaded NPs was 282 nm with a polydispersity index of 0.06 and zeta potential of 0.6 mV. The low polydispersity index (<0.1) indicates the uniform size distribution of NPs.

### Spinal cord injury:

Although of the same age, male and female rats had different body weight; an average weight of male rats was $350 \pm 6$ g, and that of female rats was $256 \pm 3$ g. The average impact force in rat studies was $243.9 \pm 3.6$ Kdyn, and the speed of the impactor was $120.7 \pm 0.4$ mm/s. All the animals developed complete paraplegia following SCI. There was no animal mortality during the experimental period in any of the groups.

### Effect of dose on localization of NPs in spinal cord:

This study was carried out in animals in which the dose of NPs was administered at 6 hrs post-injury, and the spinal cords were harvested 1 day after the injection. The signal count for each ROI was plotted to map the entire spinal cord. The data show significantly greater, and dose-dependent increased NP-specific signal at the lesion site/epicenter (segments 21 to 26) than in the remaining uninjured segments of the spinal cord (Figure 2A). The AUC for the lesion site and that for the entire spinal cord were used to determine the relative signal count for the lesion site (Figure 2B). At lower NP doses (15 and 30 mg/kg), most of the NP signal was from the lesion site (~76%); however, at higher NP dose (60 mg/kg), the signal count also increased in the areas of cervical (segments 5–11 or C4-T) and lumbar (Segments 27–32 or T11-S2) enlargement regions [21, 22] (Figure 2B) but remained significantly lower than that at the lesion site (~60% signal from Epicenter) (Table 1). The spinal cord images

show the NP-specific signal whereas the spinal cords of the animals which did not receive NPs show no such signal (Figure 2Ca vs. 2Cb). The cross-sectional views of spinal cord further confirmed the localization of NPs deep into the lesion site (Figure 2C).

Interestingly, we also noticed that the distribution of NPs in the spinal cord significantly changes following the injury. In uninjured animals (sham control), distribution of NPs was bimodal, with greater NP localization seen in the thoracic and lumbar enlargement regions of the spinal cord than in rest of the spinal cord but in animals with injury, localization of NPs was more at the lesion site whereas that in the enlargement regions was significantly reduced (Figure 3).

**Retention time of NPs at lesion site:**

In this study, a dose of NPs (30 mg/kg) was administered at 6 hrs post-injury, and the animals were sacrificed at 1 wk after the injection for spinal cord analysis. The AUC for the lesion site and the entire spinal cord from this experiment were compared to the AUC for the spinal cords that were analyzed at 1-day post-injection at the same dose (experiments from the dose-response study from above). The results show no significant difference in the AUC for the lesion site and the entire spinal cord at 1 day; however, at 1 wk this difference was significant (Figure 4).

**Effect of post-injury time of administration on localization NPs at lesion site:**

In this set of experiments, the same dose of NPs (30 mg/kg) was administered at different times post-injury, and the harvested spinal cords were analyzed for AUC at the lesion site and the entire spinal cord at 1 day after NP injection. The results show reduced localization of NPs at the lesion site with delayed post-injury NP administration. The highest signal intensity at the lesion site was seen when NPs were administered at 6 hrs post-injury, the earliest time-point in our study (Figure 5). Interestingly, localization of NPs at the lesion site or the entire spinal cord was higher at 2 wks post-injury administration than at 1 wk post-injury administration (Figure 5). Although delayed post-injury administration reduced the localization of NPs at the lesion site, there was increased uptake of NPs in the entire spinal cord when they were administered at 2 and 4 wks post-injury. This is evident from significantly increased AUC for the entire spinal cord at 2 and 4 wks time points than at 1 wk time point.

**Correlation between NP amount in spinal tissue homogenate and optical signal count:**

The optical signal count showed a linear correlation with the NP amount added in the spinal cord tissue homogenate ($R^2 = 0.99$) (Figure 6). Using this standard plot and total wet weight of the spinal cord ($125 \pm 8.9$ mg), the NP amount present in the entire spinal cord treated with 30 mg/kg dose at 6 hr post-injury and harvested at 1-day post-NP administration was $14.0 \pm 1.6$ μg. From the mapping data, the total AUC for the above treatment group was $697 \pm 93$. Therefore, 100 Units of the AUC equals to $2.0 \pm 0.7$ μg NPs. The above factor was used to determine the NP amount localized at the lesion site (segments 21–26) from the respective AUC for those segments at different doses and conditions (Table 1). Based on the NP dose injected to each animal (average weight of rat =289 g, 30 mg/kg dose or 8.7 mg/per animal), it can be estimated that $0.13 \pm 0.02\%$ of the administered NP dose localized at the

lesion site which is equivalent to $10.5 \pm 1.4$ μg NPs localizing at the epicenter for this group. Table 1 shows the % dose, and amounts of NPs localized at the epicenter in different treatment groups.

### Localization of NPs at the lesion site in the porcine model of SCI:

Similar to the rat results, the pig SCI model also showed greater localization of NPs at the lesion site than at uninured sites. The signal count of the spinal tissue collected from the lesion site was ~3 fold greater than the spinal tissue collected from uninjured sites (Figure 7).

## DISCUSSION

The most common therapeutic strategy for acute SCI condition is a neuroprotective treatment that is aimed at preventing or slowing further progression of the secondary injury cascades. In this regard, different therapeutic approaches that are either targeted at immunomodulation to prevent inflammatory response, inhibition of apoptotic pathways to prevent cell death, reducing oxidative stress to neutralize the effect of reactive oxygen species, or promoting axonal growth using different growth factors have been investigated [23]. However, most therapeutic agents either have rapid clearance and/or high degradation rate, and hence are not able to achieve and maintain therapeutic levels for a prolonged period at the lesion site. Further, repeated and/or high dosing of therapeutic agents (e.g., methylprednisone) can cause severe toxicity [24].

Recently, we reviewed several drug delivery approaches that are focused on addressing the above issues [25]. Most of these approaches are for direct injection (e.g., hydrogels, nanoparticles, nanofibers, etc.) at the lesion site but few studies have also reported the use of nanomaterials for drug delivery via intravenous injection but were given immediately or within a very short time window post-injury [26, 27]. As such, there is no systematic study aimed at analyzing the effect of different parameters that are critical for localization of NPs at the lesion site under clinically relevant conditions. In this regard, the optical imaging method that we have developed to quantitatively map the spinal cord including the lesion site for NP localization is quite sensitive and efficient, as it does not require tissue processing. The method is also useful in understanding the dynamics of distribution of NPs within the spinal cord with time. The PLGA-based NPs were used in our study as they are formulated using an FDA approved biocompatible and biodegradable polymer, and also different therapeutic agents can be encapsulated with sustained release properties. Further, depending upon the pathological need of a disease condition, the rate and duration of drug release from these can also be modulated [28].

Our data show that the localization of intravenously injected NPs at the lesion site is significantly greater than in the remaining uninjured segments of the spinal cord. Further, increasing the dose of NPs resulted in increased localization of NPs at the lesion site (Figure 2). Since contusion SCI leads to the rupture of blood vessels at the impacted site, causing the BSCB to breakdown [29], the NPs from the circulation can extravagate to the lesion site. A proportional increase in localization of NPs at the lesion site with an increasing dose of NPs (Figure 2, Table 1) is advantageous, as it provides flexibility in dose adjustment depending

upon the treatment response. Further, significantly greater localization of NPs at the lesion site than in the remaining uninjured segment gives a target-specific therapeutic intervention within the spinal cord.

Interestingly, increasing the NP dose also resulted in greater localization of NPs in the uninjured segments of the spinal cord, more specifically in the thoracic and lumbar expansion regions (Figure 2). These enlargement regions are the segments of the spinal cord where a myriad of neurons cluster to control muscular movement and other functions of the upper and lower extremities. As such, oxygen demand and hence capillary density in these areas is significantly higher than in other parts of the spinal cord [30]. It is therefore likely that more NPs are entrapped in these regions than in other regions of the spinal cord. Because of the same reason, sham control animals demonstrated greater localization of NPs in these regions than in the rest of the spinal cord (Figure 3). However, this distribution of NPs dramatically changed in the spinal cords of the animals with injury that showed greater localization of NPs at the lesion site whereas the levels in the enlargement regions were significantly reduced (Figure 3). This reduction in NP levels in the enlargement regions could be due to the post-injury ischemic condition created in the spinal cord, thus reducing the blood flow and hence the transport of NPs to the enlargement regions [31]. Thus, the overall results indicate significant hemodynamic changes in the spinal cord following the injury.

The administered NPs were seen to be retained at the lesion site, as there was no significant decline in the AUC for the lesion site at 1 day and 1 wk post-NP administration (Figure 4). Eventually, localized NPs would degrade slowly and completely because of the biodegradable nature of the polymer; however, the availability of the encapsulated drug at the lesion site would depend on its release profile from NPs. In this case, the dye is encapsulated at a very low concentration, and hence its release is minimum, and also the degradation of NPs within a week is not expected to be significant to cause their complete dissolution. We have previously shown that drug release and biodegradation of NPs could follow a different kinetic; the drug release would mainly depend upon its physical characteristics, drug loading, and the mechanism of release (diffusion plus biodegradation of polymer) whereas biodegradation of NPs would mainly depend on the polymer composition (lactide to glycolide ratio) and its molecular weight [32]. Nonetheless, the critical point is that the NPs that localize at the lesion site are retained, acting like a depot through which the encapsulated therapeutic agent would be released locally and in a sustained manner.

The data also show that there is greater diffusion of NPs in the spinal cord when analyzed at 1-wk compared to that at 1-day post-NP administration. This diffusion of NPs with time could be because of a partial resumption of blood flow to the spinal cord and/or due to increased inflammation and edema at one week, causing NPs to diffuse from the lesion site to the uninjured segments of the spinal cord [33]. It is also possible that the NPs localized in other body compartments equilibrate with the blood with time, and they then extravasate into the inflamed spinal cord.

The administration of NPs at 1-wk post-injury reduced their localization at the lesion site as compared to that seen when NPs were injected at 6 hrs post-injury (Figure 5). This reduced

localization of NPs with delayed post-injury injection time could be due to partial healing of the injured vasculature. Interestingly, there was increased localization of NPs at the lesion site when they were injected at 2-wks than at 1-wk post-injury. It is possible that inflammation is causing the BSCB to partially open-up again for greater uptake of NPs at the lesion site. It is known that macrophages, which infiltrate the lesion site following injury, may be the cause of inflammation. Injecting NPs at 4-wks post-injury reduced the localization of NPs at the lesion site as compared to that seen at 6-hr and 2-wks post-injury administration. This drop in NPs localization could be due to partial closure of the BSCB, caused by subsiding inflammation and/or due to scar tissue formation at the lesion site [34, 35]. The surprising result was the overall increased localization of NPs in the entire spinal cord when these were administered at 2- and 4-wks as compared to at1 wk post-injury (Figure 5). Although more studies are needed to understand the above phasic behavior of NP localization in the spinal cord, it is known that different events occur in a phasic pattern following SCI, which either overlap or occur in a sequential pattern [34, 35]. For example, Figley et al. [36] have reported time-dependent phasic changes in the BSCB permeability and revascularization, not only at the lesion site but also distal to the lesion site. Nonetheless, one critical finding from this study was that even after 4 wks post-injury, the BSCB at the lesion site remains accessible to the intravenously injected NPs. However, the localization of NPs in the spinal cord could change if these are encapsulated with a therapeutic agent and its mechanism of action. Interesting would be to explore the dye and drug-loaded NPs to determine how the incorporated drug influences the mobility of NPs within the spinal cord and/or their uptake to analyze the treatment effect on spinal cord inflammation, change in the BSCB permeability, and overall healing of the spinal cord.

Similar to the rat results, we observed greater localization of NPs at the lesion site in the pig contusion model of SCI (Figure 7). Kwon et al. have developed and extensively characterized this pig model of SCI for locomotor recovery and also physiologic and biochemical responses to injury [39].

Based on the 30 mg/kg dose injected 6 hrs post-injury and spinal cord analyzed at 1-day post-NP administration, it is estimated that ~0.13% of the injected NP dose localizes at the lesion site. However, as shown in Table 1, various factors influence the dose and efficiency of localization of NPs at the lesion site. It is anticipated that the lesion site, depending upon the injury volume would have a limited holding capacity for the injected NPs; therefore, the critical consideration while developing a treatment for SCI is the potency of therapeutic agents so that the dose delivered to the lesion site is effective.

Although we did not determine biodistribution of NPs in this study, previously we have shown in mice with a similarly formulated dye-loaded NPs that they localize in other body compartments including in the liver, spleen, lung, and kidney [17]. However, the major fraction of the administered dose was seen to be eliminated from the body in ~4 days, presumably via the biliary duct to the gut [37]. In this study, we show that the NPs are retained at the lesion site for more than a week without significant change from 1 day to 1 week (Figure 4). This is advantageous as the NPs at the lesion site will be retained for a longer period of time whereas those in other body compartments will be eliminated, minimizing the risk of non-specific effect. In addition, it is known that apart from local

injury within the spinal cord, SCI patients are characterized by multiple organ dysfunction or failure, due to marked increase in circulation of immune cells, pro-inflammatory mediators, and free radicals [38]. Hence, in addition to protecting spinal cord, the NPs localized in other organs can also have a protective effect. For example, NPs loaded with anti-inflammatory agents or antioxidants could provide protective effect to both the spinal cord and other organs. A significant advantage of using NPs as a drug carrier is that the drug effect at the lesion site can be substantially prolonged as compared to that when drugs are given as a solution. Sustained drug effect at the lesion site with NPs vs. transient effect with solution can potentially influence the short- and long-term therapeutic outcome. Also, it cannot be ruled out that the NPs retained at the lesion site acting as a scaffold, providing a support structure to facilitate neuronal regrowth and regeneration.

Direct injection of NPs to the lesion site has been tested as a therapeutic approach for SCI. For example, Chvatal et al. have shown that the PLGA-NPs encapsulating methylprednisolone were effective in controlling inflammation and reducing the lesion cavity in a rat model of contusion SCI [40]. However, the study was carried out by injecting NPs immediately following inducing SCI which is not a clinically relevant scenario but useful to demonstrate that the localized and sustained drug effect is effective than one may see with a transient effect with drugs administered as a solution.

Considering the degenerative nature of the secondary injury cascade that rapidly progresses with time following the injury, therapeutic intervention is sought that can be administered as soon as possible post-injury including at the site of incidence or *en route* to a trauma center. The timely intervention is especially critical in a battlefield condition where resources are limited, requiring victims to be transported to a nearby military base; victims may suffer from other life-threatening conditions that may require urgent attention; or in rural areas where a trauma center may be far away from the site of incidence. Although direct injection of NPs to the spinal cord could be more efficient than the intravenous injection in localizing the treatment to the spinal cord, it cannot be carried out under the above circumstances and within a short period of time post-injury. Hence, our focus has been on developing an intravenously injectable formulation that can be administered under the above conditions, potentially at the site of incidence to inhibit the rapidly progressing post-injury secondary injury cascade. Besides, repeated treatment may be needed with the same or a combination of a therapeutic agent(s) during the chronic phase to facilitate the regeneration of the injured spinal cord. Recently, Anderson et al. [41] have shown that a combination of growth factors delivered in sequential order via hydrogel applied directly to a completely transected spinal cord is needed for robust axonal regrowth across the site of the incision. In this regard, NPs could provide an effective drug carrier system that can be administered at different time-points post-injury to minimize the impact of the injury response as well during the regenerative phase carrying different therapeutic agents.

## CONCLUSIONS

Our data demonstrate that following their intravenous injection, NPs localize at the lesion site in a dose-dependent manner within a wide time window post-injury. Further, such NPs are retained at the lesion site for a sustained period. The delay in injecting NPs post-injury

reduces their localization at the lesion site; however, the BSCB at the lesion site remains accessible to the intravenously administered NPs for a prolonged period of time following the injury. Due to their sustained release properties, NPs can potentially provide early as well prolonged drug effect at the lesion site that can impact short- and long-term outcomes. Further, different pathways for post-injury degeneration of spinal cord have been under investigation, and these could be phasic or sequential. Thus, one could potentially time NP delivery so that a particular pathway or pathways active at that time could be targeted to intervene in the cascade of spinal cord degeneration.

## Acknowledgment:

## Abbreviations

| | |
|---|---|
| **BSCB** | Blood-spinal cord barrier |
| **IV** | Intravenously |
| **NIR** | Near-infrared |
| **NPs** | Nanoparticles |
| **PLGA** | Poly (D,L-lactide $co$-glycolide) |
| **PVA** | Poly (vinyl alcohol) |
| **rpm** | Rotations per minute |
| **SCI** | Spinal cord injury |

## Bibliography

[1]. Lee YS, Lin CY, Jiang HH, Depaul M, Lin VW, Silver J, Nerve regeneration restores supraspinal control of bladder function after complete spinal cord injury, J Neurosci, 33 (2013) 10591–10606. [PubMed: 23804083]

[2]. Kuzhandaivel A, Nistri A, Mazzone GL, Mladinic M, Molecular Mechanisms Underlying Cell Death in Spinal Networks in Relation to Locomotor Activity After Acute Injury in vitro, Frontiers in cellular neuroscience, 5 (2011) 1–17. [PubMed: 21286222]

[3]. Crowe MJ, Bresnahan JC, Shuman SL, Masters JN, Beattie MS, Apoptosis and delayed degeneration after spinal cord injury in rats and monkeys, Nat Med, 3 (1997) 73–76. [PubMed: 8986744]

[4]. Lu J, Ashwell KW, Waite P, Advances in secondary spinal cord injury: role of apoptosis, Spine, 25 (2000) 1859–1866. [PubMed: 10888960]

[5]. Springer JE, Azbill RD, Knapp PE, Activation of the caspase-3 apoptotic cascade in traumatic spinal cord injury, Nat Med, 5 (1999) 943–946. [PubMed: 10426320]

[6]. Oyinbo CA, Secondary injury mechanisms in traumatic spinal cord injury: a nugget of this multiply cascade, Acta Neurobiol Exp (Warsz), 71 (2011) 281–299. [PubMed: 21731081]

[7]. Liu XZ, Xu XM, Hu R, Du C, Zhang SX, McDonald JW, Dong HX, Wu YJ, Fan GS, Jacquin MF, Hsu CY, Choi DW, Neuronal and glial apoptosis after traumatic spinal cord injury, J Neurosci, 17 (1997) 5395–5406. [PubMed: 9204923]

[8]. Watson R, Yeung T, What is the potential of oligodendrocyte progenitor cells to successfully treat human spinal cord injury?, BMC Neurol, 11 (2011) 113. [PubMed: 21943254]

[9]. Fehlings MG, Perrin RG, The role and timing of early decompression for cervical spinal cord injury: update with a review of recent clinical evidence, Injury, 36 Suppl 2 (2005) B13–26. [PubMed: 15993113]

[10]. Thuret S, Moon LD, Gage FH, Therapeutic interventions after spinal cord injury, Nat Rev Neurosci, 7 (2006) 628–643. [PubMed: 16858391]

[11]. Guercio JR, Kralic JE, Marrotte EJ, James ML, Spinal cord injury pharmacotherapy: Current research & development and competitive commercial landscape as of 2015, J. Spinal Cord Med 42(2019) 102–12. [PubMed: 29485334]

[12]. Schomberg DT, Miranpuri GS, Chopra A, Patel K, Meudt JJ, Tellez A, Resnick DK, Shanmuganayagam D, Translational Relevance of Swine Models of Spinal Cord Injury, J Neurotrauma, 34 (2017) 541–551. [PubMed: 27492951]

[13]. Reddy MK, Wu L, Kou W, Ghorpade A, Labhasetwar V, Superoxide dismutase-loaded PLGA nanoparticles protect cultured human neurons under oxidative stress, Appl Biochem Biotechnol, 151 (2008) 565–577. [PubMed: 18509606]

[14]. Singhal A, Morris VB, Labhasetwar V, Ghorpade A, Nanoparticle-mediated catalase delivery protects human neurons from oxidative stress, Cell Death Dis, 4 (2013) e903. [PubMed: 24201802]

[15]. Estey T, Kang J, Schwendeman SP, Carpenter JF, BSA degradation under acidic conditions: a model for protein instability during release from PLGA delivery systems, J Pharm Sci, 95 (2006) 1626–1639. [PubMed: 16729268]

[16]. Reddy MK, Labhasetwar V, Nanoparticle-mediated delivery of superoxide dismutase to the brain: an effective strategy to reduce ischemia-reperfusion injury, Faseb j, 23 (2009) 1384–1395. [PubMed: 19124559]

[17]. Adjei IM, Peetla C, Labhasetwar V, Heterogeneity in nanoparticles influences biodistribution and targeting, Nanomedicine (London, England), 9 (2014) 267–278.

[18]. Stees M, Adjei I, Labhasetwar V, A Method for Quantification of Penetration of Nanoparticles through Skin Layers Using Near-Infrared Optical Imaging, Cosmetics, 2 (2015) 225.

[19]. Lee JH, Jones CF, Okon EB, Anderson L, Tigchelaar S, Kooner P, Godbey T, Chua B, Gray G, Hildebrandt R, Cripton P, Tetzlaff W, Kwon BK, A novel porcine model of traumatic thoracic spinal cord injury, J Neurotrauma, 30 (2013) 142–159. [PubMed: 23316955]

[20]. Nair AB, Jacob S, A simple practice guide for dose conversion between animals and human, J Basic Clin Pharm, 7 (2016) 27–31. [PubMed: 27057123]

[21]. Portiansky EL, Nishida F, Barbeito CG, Gimeno EJ, Goya RG, Increased number of neurons in the cervical spinal cord of aged female rats, PLoS One, 6 (2011) e22537. [PubMed: 21799890]

[22]. Harrison M, O'Brien A, Adams L, Cowin G, Ruitenberg MJ, Sengul G, Watson C, Vertebral landmarks for the identification of spinal cord segments in the mouse, Neuroimage, 68 (2013) 22–29. [PubMed: 23246856]

[23]. Karsy M, Hawryluk G, Pharmacologic Management of Acute Spinal Cord Injury, Neurosurg Clin N Am, 28 (2017) 49–62. [PubMed: 27886882]

[24]. Evaniew N, Belley-Côté EP, Fallah N, Noonan VK, Rivers CS, Dvorak MF, Methylprednisolone for the Treatment of Patients with Acute Spinal Cord Injuries: A Systematic Review and Meta-Analysis, J Neurotrauma, 33 (2016) 468–481. [PubMed: 26529320]

[25]. Kabu S, Gao Y, Kwon BK, Labhasetwar V, Drug delivery, cell-based therapies, and tissue engineering approaches for spinal cord injury, J Control Release, 219 (2015) 141–154. [PubMed: 26343846]

[26]. Macks C, Gwak SJ, Lynn M, Lee JS, Rolipram-Loaded Polymeric Micelle Nanoparticle Reduces Secondary Injury after Rat Compression Spinal Cord Injury, J Neurotrauma, 35 (2018) 582–592. [PubMed: 29065765]

[27]. Papa S, Caron I, Erba E, Panini N, De Paola M, Mariani A, Colombo C, Ferrari R, Pozzer D, Zanier ER, Pischiutta F, Lucchetti J, Bassi A, Valentini G, Simonutti G, Rossi F, Moscatelli D, Forloni G, Veglianese P, Early modulation of pro-inflammatory microglia by minocycline loaded nanoparticles confers long lasting protection after spinal cord injury, Biomaterials, 75 (2016) 13–24. [PubMed: 26474039]

[28]. Panyam J, Labhasetwar V, Biodegradable nanoparticles for drug and gene delivery to cells and tissue, Adv Drug Deliv Rev, 55 (2003) 329–347. [PubMed: 12628320]

[29]. Maikos JT, Shreiber DI, Immediate damage to the blood-spinal cord barrier due to mechanical trauma, J Neurotrauma, 24 (2007) 492–507. [PubMed: 17402855]

[30]. Nystrom B, Stjernschantz J, Smedegard G, Regional spinal cord blood flow in the rabbit, cat and monkey, Acta Neurol Scand, 70 (1984) 307–313. [PubMed: 6507040]

[31]. Streijger F, So K, Manouchehri N, Tigchelaar S, Lee JHT, Okon EB, Shortt K, Kim SE, McInnes K, Cripton P, Kwon BK, Changes in Pressure, Hemodynamics, and Metabolism within the Spinal Cord during the First 7 Days after Injury Using a Porcine Model, J Neurotrauma, 34 (2017) 3336–3350. [PubMed: 28844181]

[32]. Panyam J, Dali MM, Sahoo SK, Ma W, Chakravarthi SS, Amidon GL, Levy RJ, Labhasetwar V, Polymer degradation and in vitro release of a model protein from poly(d,l-lactide-co-glycolide) nano- and microparticles, J Control Release, 92 (2003) 173–187. [PubMed: 14499195]

[33]. Anwar MA, Al Shehabi TS, Eid AH, Inflammogenesis of Secondary Spinal Cord Injury, Front Cell Neurosci, 10 (2016) 98. [PubMed: 27147970]

[34]. Beck KD, Nguyen HX, Galvan MD, Salazar DL, Woodruff TM, Anderson AJ, Quantitative analysis of cellular inflammation after traumatic spinal cord injury: evidence for a multiphasic inflammatory response in the acute to chronic environment, Brain, 133 (2010) 433–447. [PubMed: 20085927]

[35]. Golovatscka V, Ennes H, Mayer EA, Bradesi S, Chronic stress-induced changes in pro-inflammatory cytokines and spinal glia markers in the rat: a time course study, Neuroimmunomodulation, 19 (2012) 367–376. [PubMed: 23051934]

[36]. Figley SA, Khosravi R, Legasto JM, Tseng YF, Fehlings MG, Characterization of vascular disruption and blood-spinal cord barrier permeability following traumatic spinal cord injury, J Neurotrauma, 31 (2014) 541–552. [PubMed: 24237182]

[37]. Adjei IM, Sharma B, Peetla C, Labhasetwar V, Inhibition of bone loss with surface-modulated, drug-loaded nanoparticles in an intraosseous model of prostate cancer, J Control Release, 232 (2016) 83–92. [PubMed: 27090164]

[38]. Sun X, Jones ZB, Chen XM, Zhou L, So KF, Ren Y, Multiple organ dysfunction and systemic inflammation after spinal cord injury: a complex relationship, J Neuroinflammation, 13 (2016) 260. [PubMed: 27716334]

[39]. Streijger F, Lee JH, Chak J, Dressler D, Manouchehri N, Okon EB, Anderson LM, Melnyk AD, Cripton PA, Kwon BK, The effect of whole-body resonance vibration in a porcine model of spinal cord injury, J Neurotrauma, 32 (2015) 908–921. [PubMed: 25567669]

[40]. Chvatal SA, Kim YT, Bratt-Leal AM, Lee H, Bellamkonda RV, Spatial distribution and acute anti-inflammatory effects of Methylprednisolone after sustained local delivery to the contused spinal cord, Biomaterials, 29 (2008) 1967–1975. [PubMed: 18255138]

[41]. Anderson MA, O'Shea TM, Burda JE, Ao Y, Barlatey S, Bernstein L,,A, Kim M,J, James H,ND, Rogers A, Kato B, Wollenberg AL, Kawaguchi R, Coppola G, Wang C, Deming TJ, He Z, Courtine G, Sofroniew MV, Required growth facilitators propel axon regeneration across complete spinal cord injury., Nature, 561 (2018) 396–400. [PubMed: 30158698]
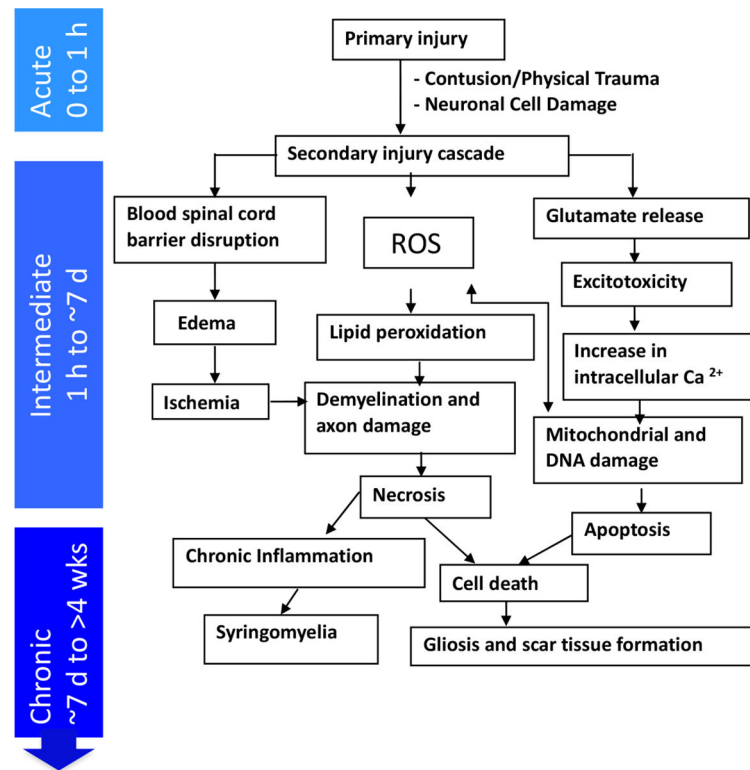
**Figure 1: Progression of spinal cord injury response.**
A depiction of the progression of degenerative events with time following SCI. The intermediate phase provides a window of treatment to minimize the impact of secondary injury cascade.
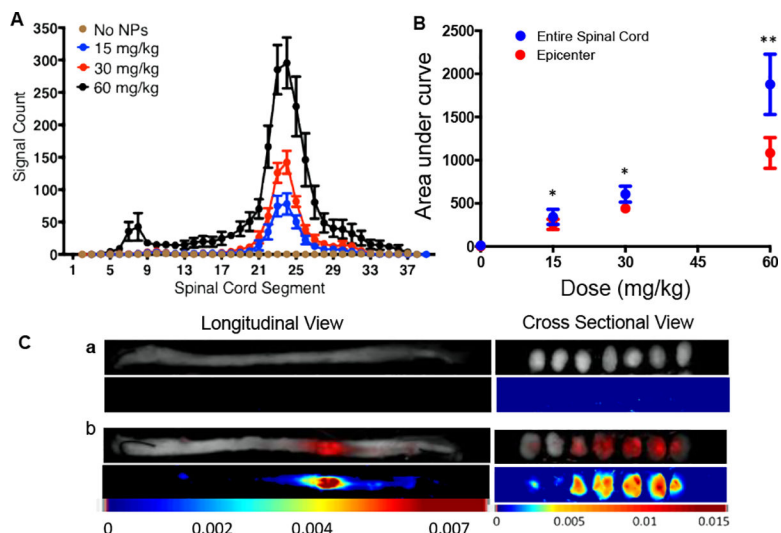
**Figure 2: Effect of dose of NPs on their localization at the lesion site.**
Different doses of NPs were administered via tail vein at 6 hr post-injury, and spinal cords were harvested 24 hrs post-NP injection. The mapping of the spinal cord for the signal count was carried out using the Maestro Optical Imaging System. **A)** Dose-dependent change in signal intensity along the entire spinal cord including the lesion site. The lesion site shows significantly greater signal intensity than the uninjured site. Data as mean ± s.e.m., n= 6 to 7. **B)** The AUC calculated from the mapping of the entire spinal cord and the lesion site (segments C21 to C26). The data show dose-dependent increased localization of NPs at the lesion site. Data as mean ± s.e.m, n=6 to 7. Differences in signal count for entire spinal cord vs. epicenter at 15 and 30 mg/kg, *p<0.05 and at 60 mg/kg, **p<0.01. Differences in AUC between the doses for both epicenter and entire spinal cord p = 0.01. **C)** Representative images of the spinal cord of a) control animals which did not receive NPs and b) animals that received NP injection, showing greater localization of NPs at the lesion site than in uninured segments. Representative cross-sectional views show localization of NPs deep into the lesion site whereas spinal cords of control animals that did not receive NPs show no NP-specific signal. Shown are sections from the epicenter and representative sections rostral and cranial ends.
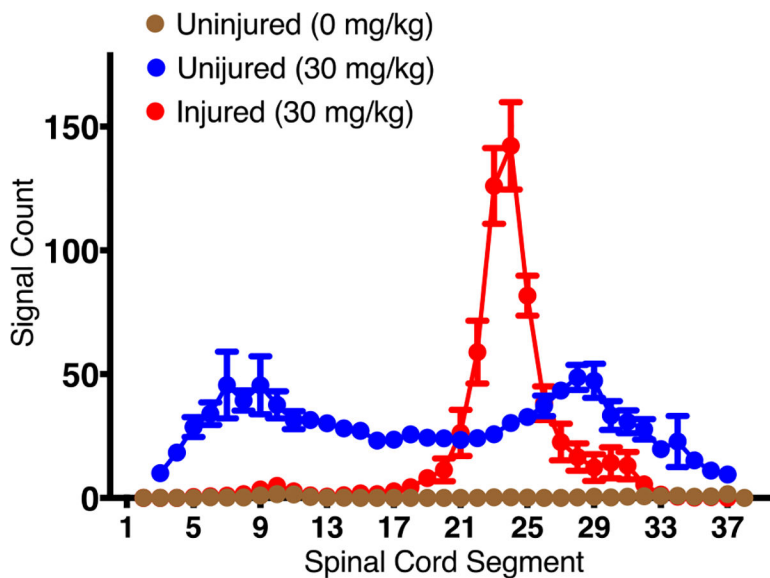
**Figure 3: Dynamics of changes in NP localization following SCI.**
Animals with and without SCI injury were injected NPs. The data show a bimodal distribution of NPs in sham control animals whereas, in injured animals, localization of NPs was seen primarily at the lesion site. Data as mean ± s.e.m., n=6
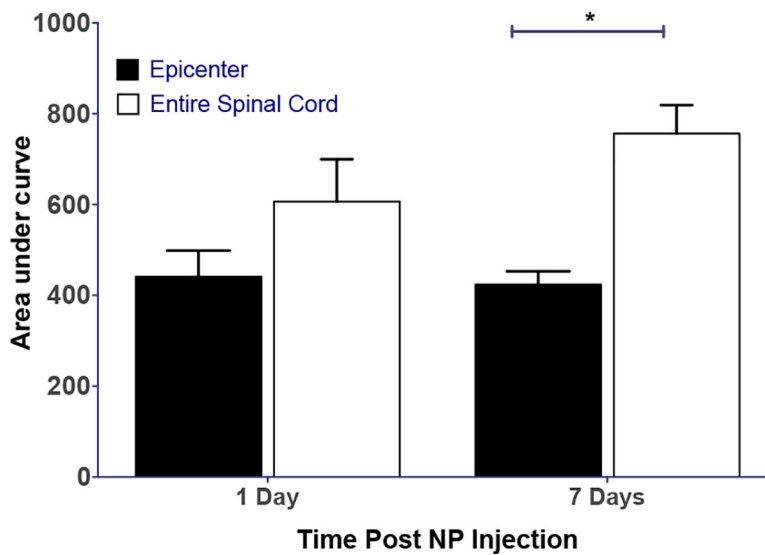
**Figure 4: Retention of NPs at the lesion site following post-injury administration.**
NPs were (30 mg/kg) administered at 6 hrs post-injury, and spinal cords were harvested for mapping either at 1-day or 1-wk post-NP injection. NPs are seen to be retained at the lesion site over 1 wk. Data as mean ± s.e.m., n=6. *p<0.01. NS= 1-day epicenter vs. entire spinal cord; NS=1-day vs. 7-day epicenter or entire spinal cord.
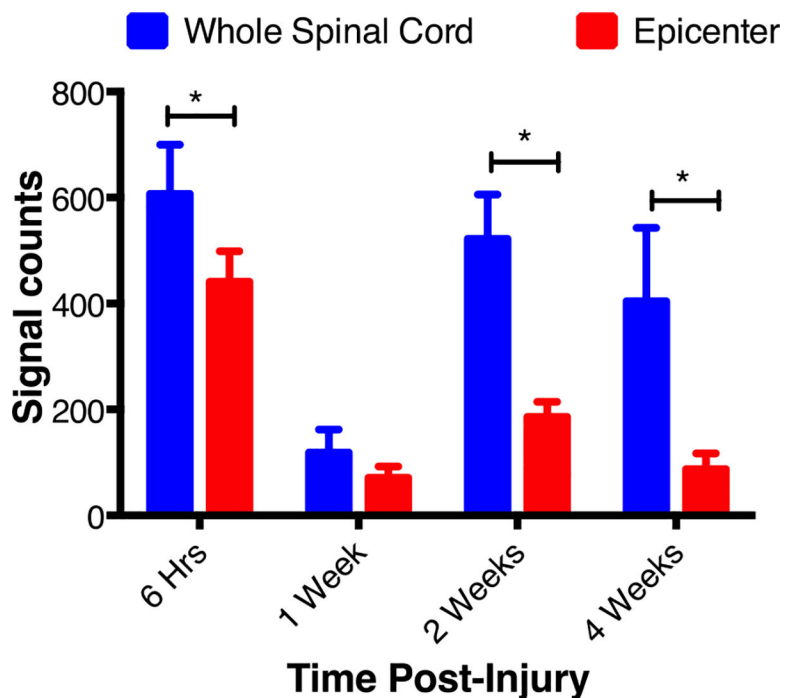
**Figure 5: Effect of time post-injury administration of NPs on the localization of NPs at the lesion site.**

NPs were injected at different time point post-injury, and spinal cords were harvested 24 hrs post-NP injection. The AUC shows a phasic change in the localization of NPs. At earlier time points (6 hr and 1 wk), NP localization was seen mostly at the epicenter whereas, at later time points (2 and 4 wks), there is greater localization of NPs in the entire spinal cord as compared to that at the epicenter. Data as mean ± s.e.m, n= 5 to 6. Difference in the AUC between epicenter and entire spinal cord *p<0.05 but NS at 1-wk. Differences in the AUC for the entire spinal cord and epicenter with time p<0.05.
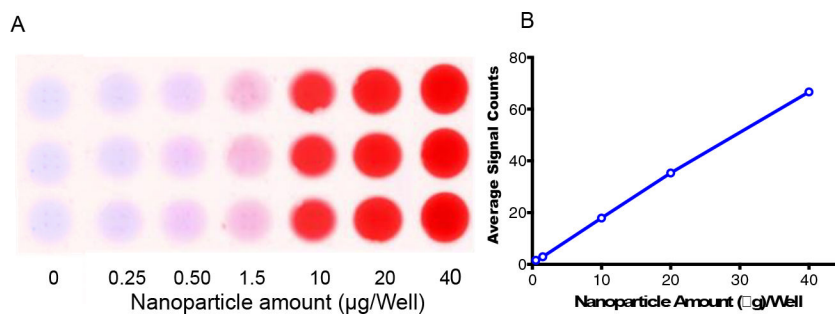
**Figure 6: Correlation between signal counts and NP amount in spinal tissue homogenate.** Different amounts of NPs were added to spinal tissue homogenate, and the signal count was measured. The relation between NPs added, and the signal count is linear. **A)** Optical image of the well loaded with different amounts of NPs added into spinal cord homogenate, **B)** Linear co-relation between signal count and NP amount added in spinal cord homogenate. $R^2 = 0.99$, Data as mean ± s.e.m., n=3. Error bars are smaller than the size of symbols.
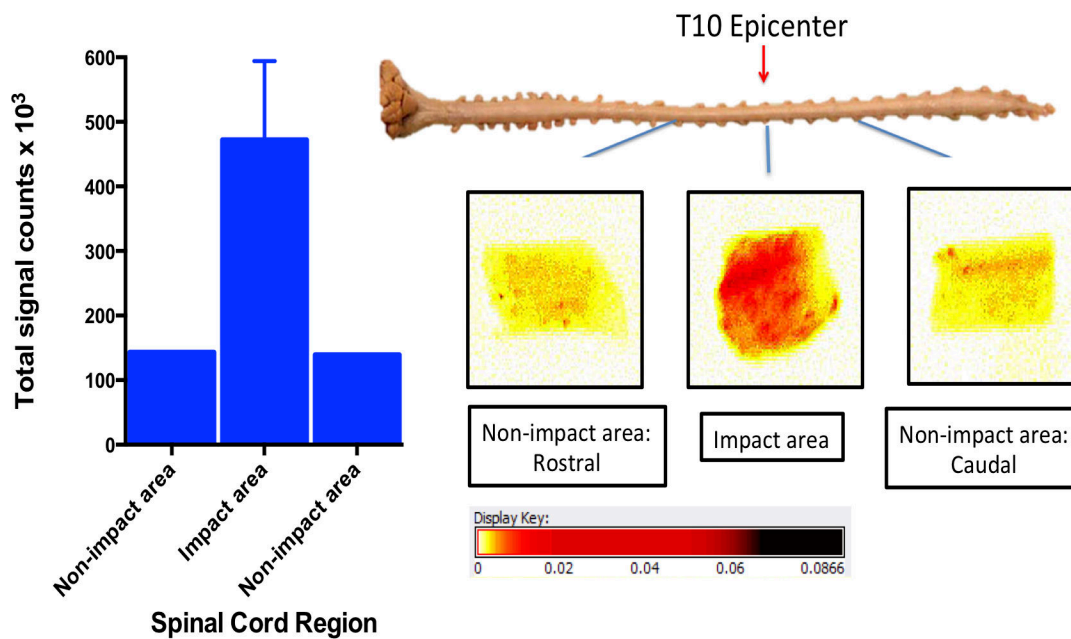
**Figure 7: Localization of NP at the lesion site in the pig model of SCI.**
The dye-loaded NPs were injected IV (8 mg/kg in 20 ml saline) 3 hrs post-contusion injury, the spinal cord sections from the impact and non-impact sites were harvested 2 hrs following NP injection and imaged using Maestro. Images are longitudinal pieces (not cross sections) of the spinal cord. Four pieces were cut from the lesion site and one each from caudal and rostral sites. Data shown for the lesion site are mean ± s.e.m. of four pieces of tissue collected from the lesion site. In another animal, NPs were injected 30 min post-injury, and the spinal cord was harvested 5 hrs post-NP injection which also showed similar greater uptake at the lesion site (data not shown).

**Table 1:**

Effect on different parameters on localization of NPs at impacted site

| A: Effect of dose: NPs administered at 6 hrs post-injury and spinal cords were analyzed at 24 hrs post-injection | | | | | |
|---|---|---|---|---|---|
| Dose | AUC for entire spinal cord | AUC for Epicenter | % at Epicenter compared to entire spinal cord | % administered NP dose localized at epicenter | NP amount localized at Epicenter (μg) |
| 15 mg/kg | 343 ± 87 | 256 ± 59 | 77.2 ± 3.1 | 0.15 ± 0.04 | 6.08 ± 1.4 * |
| 30 mg/kg | 697 ± 92 | 441 ± 58 | 74.8 ± 4.3 | 0.13 ± 0.02 | 10.49 ± 1.4 |
| 60 mg/kg | 1878 ±35 | 1084 ± 18 | 60.5 ±3.7 | 0.08 ± 0.01 | 14.29 ± 1.1 |
| B: Effect of time post-injury NP administration: dose of NPs =30 mg/kg and spinal cords were analyzed at 24 hrs post-injection | | | | | |
| 6 hr | 697 ± 92 | 441 ± 58 | 74.8 ± 4.3 | 0.13 ± 0.017 | 10.49 ± 1.4 ** |
| 1 wk | 119 ± 43 | 71 ± 21 | 71.3 ± 8.9 | 0.021 ± 0.006 | 1.69 ± 0.5 |
| 2 wk | 533 ± 83 | 185 ± 28 | 35.8 ± 0.9 | 0.027 ± 0.004 | 2.05 ± 0.3 |
| 4 wk | 652 ± 83 | 87 ± 30 | 22.7 ± 3.5 | 0.009 ± 0.003 | 0.77 ± 0.2 |
| C: Retention of N Ps: dose of NPs =30 mg/kg; injected at 6 and spinal cords were analyzed either at 24 hrs or 1 wk post-injection | | | | | |
| 1 day | 697 ± 92 | 441 ± 58 | 74.8 ± 4.3 | 0.13 ± 0.02 | 10.49 ± 1.4 *** |
| 1 wk | 756 ± 62 | 423 ± 29 | 56.5 ± 1.8 | 0.113 ± 0.03 | 10.08 ± 0.7 |

Data as mean ± s.e.m, n= 5–6. Includes both male and female rats.

*
A: $p < 0.05$ (two tailed) between doses;

**
B: $p < 0.05$ (two tailed) between different time points;

***
C: $p < 0.0001$